BIOCHEMISTRY
including biophysical chemistry & molecular biology
Article

Biochemistry **2010,** *49,* 8169–8176 8169
DOI: 10.1021/bi101146v

Role of the Highly Conserved Middle Region of Prion Protein (PrP) in PrP−Lipid Interaction†

Fei Wang,‡ Shaoman Yin,§ Xinhe Wang,‡ Liang Zha,‡ Man-Sun Sy,§ and Jiyan Ma*,‡

‡*Department of Molecular and Cellular Biochemistry, The Ohio State University, Columbus, Ohio 43210, and*
§*Department of Pathology and Department of Neurosciences, Case Western Reserve University School of Medicine, Cleveland, Ohio 44106*

Received July 19, 2010; Revised Manuscript Received August 16, 2010

ABSTRACT: Converting normal prion protein (PrP^C) to the pathogenic PrP^{Sc} isoform is central to prion disease. We previously showed that, in the presence of lipids, recombinant mouse PrP (rPrP) can be converted into the highly infectious conformation, suggesting a crucial role of lipid−rPrP interaction in PrP conversion. To understand the mechanism of lipid−rPrP interaction, we analyzed the ability of various rPrP mutants to bind anionic lipids and to gain lipid-induced proteinase K (PK) resistance. We found that the N-terminal positively charged region contributes to electrostatic rPrP−lipid binding but does not affect lipid-induced PK resistance. In contrast, the highly conserved middle region of PrP, consisting of a positively charged region and a hydrophobic domain, is essential for lipid-induced rPrP conversion. The hydrophobic domain deletion mutant significantly weakened the hydrophobic rPrP−lipid interaction and abolished the lipid-induced C-terminal PK resistance. The rPrP mutant without positive charges in the middle region reduced the amount of the lipid-induced PK-resistant rPrP form. Consistent with a critical role of the middle region in lipid-induced rPrP conversion, both disease-associated P105L and P102L mutations, localized between lysine residues in the positively charged region, significantly affected lipid-induced rPrP conversion. The hydrophobic domain-localized 129 polymorphism altered the strength of hydrophobic rPrP−lipid interaction. Collectively, our results suggest that the interaction between the middle region of PrP and lipids is essential for the formation of the PK-resistant conformation. Moreover, the influence of disease-associated PrP mutations and the 129 polymorphism on PrP−lipid interaction supports the relevance of PrP−lipid interaction to the pathogenesis of prion disease.

Prion diseases constitute a group of transmissible neurodegenerative disorders, including Creutzfeldt-Jakob disease (CJD)[1] and Gerstmann-Straussler-Scheinker syndrome (GSS) in humans, scrapie in sheep, and bovine spongiform encephalopathy in cows (*1*−*3*). The transmission of prion disease is mediated by an unusual infectious agent, which is composed of a pathogenic conformer of the normal prion protein (PrP) (*1*, *4*−*6*). The conformational change of PrP, converting the normal protease-sensitive PrP^C to the pathogenic protease-resistant PrP^{Sc} form, is a critical pathogenic event in prion disease (*7*−*11*). We recently reported that in the presence of anionic phospholipid POPG (1-palmitoyl-2-oleoylphosphatidylglycerol) and total mouse liver RNA, bacterially expressed recombinant PrP (rPrP) can be converted in vitro into the infectious conformer, causing prion disease in wild-type animals (*12*). The high prion infectivity associated with the recombinant prion highlights a critical role of POPG and RNA in converting rPrP into the infectious conformation (*13*).

The facilitating role of factors such as phospholipid and RNA in PrP conversion is consistent with previous reports. It has been shown that polyanions, particularly RNA molecules, enhance the in vitro propagation of naturally occurring prions (*14*, *15*). Using purified hamster PrP^C, Deleault et al. (*16*) reported that the infectious prion can be formed de novo in the presence of synthetic poly(A) RNA. Notably, the purified PrP^C used in that study contains a stoichiometric amount of copurified lipid molecules, indicating a role of lipid in PrP conversion (*16*). The role of lipid in PrP conversion has also been revealed by several previous studies. The highly purified "prion rod" contains lipid molecules (*17*), and reincorporation of prion rod into lipid vesicles results in a higher prion infectivity (*18*). Compared to detergent-purified PrP^{Sc}, the lipid membrane-associated PrP^{Sc} infects cultured cells with a higher efficiency (*19*). Altering the lipid composition of prion-infected cells affects the amount of PrP^{Sc} produced in these cells (*20*, *21*). Moreover, a glycosylphosphatidylinositol (GPI) anchor-independent PrP−lipid interaction has been found to be essential for PrP conversion in vitro (*22*). These observations are consistent with the notion that PrP−lipid interaction plays a critical role in PrP conversion.

†This work is supported by grants from the Ellison Medical Foundation and National Institutes of Health Grant R01NS060729.

*To whom correspondence should be addressed: Department of Molecular and Cellular Biochemistry, The Ohio State University, 1645 Neil Ave., Columbus, OH 43210. Fax: (614) 292-4118. Phone: (614) 688-0408. E-mail: ma.131@osu.edu.

[1]Abbreviations: PrP, prion protein; PK, proteinase K; rPrP, recombinant mouse PrP; CJD, Creutzfeldt-Jakob disease; GSS, Gerstmann-Straussler-Scheinker syndrome; GPI, glycosylphosphatidylinositol; CC1, positively charged cluster 1; CC2, positively charged cluster 2; ΔH, recombinant mouse PrP with amino acid residues 111−131 deleted; K/I, recombinant mouse PrP in which lysine residues at positions 100, 103, 105, and 109 were replaced with isoleucines; rhPrP, recombinant human PrP; ΔCC1, recombinant human PrP without the five very N-terminal amino acids; P105L, recombinant human PrP with a leucine at position 105; P102L, recombinant human PrP with a leucine at position 102; MBL, total mouse brain lipids; POPG, 1-palmitoyl-2-oleoyl-*sn*-glycero-3-phospho(1′-*rac*-glycerol) (sodium salt); POPC, 1-palmitoyl-2-oleoyl-*sn*-glycero-3-phosphocholine; Suf, sulfatides (brain): cerebroside (brain, porcine) (ammonium salt).

Published on Web 08/19/2010

The PrP−lipid interaction has been studied mainly using biophysical approaches. It has been shown that rPrP binds to lipids and the binding alters secondary structures (*23*−*27*) and destabilizes the C-terminal part of PrP (*23*). With additional treatments, lipid-bound rPrP was found to form amyloid fibers (*25*, *27*). It has also been shown that concentrated GPI-anchored PrP on a raft-like membrane domain induces PrP to form intermolecular β-sheets (*28*). We previously reported that anionic lipid−rPrP interaction converts rPrP to a conformation similar to the pathogenic PrP^{Sc} conformation, with increased β-sheet content and C-terminal PK resistance (*29*). These findings revealed that PrP binds to certain types of lipids in a manner independent of its GPI anchor, and the lipid interaction leads to conformational changes in PrP. However, it remains unclear which regions of PrP are involved in the lipid interaction, which residues of PrP are critical in converting rPrP into the PrP^{Sc}-like PK-resistant conformation, and whether disease-associated mutations affect PrP−lipid interaction. Given the role of anionic POPG in the conversion of rPrP into the highly infectious form (*12*), answers to these questions will help us to elucidate the molecular mechanism of PrP conversion.

In this study, we dissected the lipid−PrP interaction by using various rPrP mutants to compare their lipid binding ability and the lipid-induced C-terminal PK resistance. We found that the highly conserved middle region of PrP, consisting of a positively charged region with four lysine residues (amino acids 100−110) followed by a hydrophobic domain (amino acids 111−134), is crucial for lipid-induced rPrP conformational change. The middle region-localized disease-associated P102L and P105L mutations and the 129 polymorphism have distinct effects on rPrP−lipid interaction. Collectively, these results provide additional support for the relevance of PrP−lipid interaction to the pathogenesis of prion disease.

EXPERIMENTAL PROCEDURES

Primers. The following primers were used: 23BamHI, 5′-AAAGGATCCAAAAAGCGGCCAAAGCCTGGA-3′; 120HindIII, 5′-CCCAAGCTTATACTGCCCCAGCTGCCGCAGC-3′; 121BamHI, 5′-TTTGGATCCGTGGGGGGCCTTGGTGGCTAC-3′; 230RHindIII, 5′-CCCAAGCTTAGGATCTTCTCCCGTCGTAATA-3′; DELN, 5′-ACGTGCATGCTTGAGGTTGGTTTTTGG-3′; DELC, 5′-ACATGCATGCCATGAGCAGGCCCATGATCC-3′; 1MF, 5′-AATCAGTGGAACATACCAGCATACCAAAAACCAACCTC-3′; 1MR, 5′-GAGGTTGGTTTTTGGTATGCTGGGTATGTTCCACTGATT-3′; 2MF, 5′-CCCAGCATACCAATAACCAACCTCATACATGTGGCAGGG-3′; 2MR, 5′-CCCTGCCACATGTATGAGGTTGGTTATTGGTATGCTGGG-3′.

Generation of PrP Mutants. DNA fragments of mouse PrP23−120 and PrP121−230 were amplified using primers 23BamHI and 120HindIII, and 121BamHI and 230RHindIII, respectively. PCR products were then cloned into expression vector pPROEX-HTb (Invitrogen) using restriction endonucleases BamHI and HindIII. To generate mutant ΔH, the mouse PrP23−110 DNA sequence was amplified using primers 23BamHI and DELN and then linked to the EcoRV site of the pBluescript (SK) vector. The mouse PrP132−230 DNA sequence was amplified using primers DELC and 230HindIII and then linked to pBluescript (SK)-PrP23−110 via SphI and HindIII sites to generate the pBluescript (SK)-ΔH plasmid. The ΔH DNA sequence was cut off from the pBluescript vector by BamHI and HindIII and linked to pPROEX-HTb. All mutant DNA sequences in pPROEX-HTb are behind a linker sequence encoding six histidines. The histidine tag is followed by a tobacco etch virus (TEV) protease cleavage site; after TEV protease cleavage of the histidine tag, only one extra amino acid, glycine, remained at the N-terminus of PrP. For K/I, primers 1MF and 1MR were used first to mutate lysine residues at positions 100 and 103 to isoleucine residues with pPROEX-HTb-mosue PrP23−230 as a template; then primers 2MF and 2MR were used to mutate the lysine residues at positions 105 and 109 to isoleucine residues using the previously mutated plasmid as a template. The generation of human PrP mutants ΔCC1, P102L, P105L, and 129V was described previously (*30*).

Recombinant PrP Expression and Purification. Recombinant mouse PrP23−230, PrP23−120, PrP121−230, ΔH, K/I, and recombinant human PrPs were purified as previously described (*31*, *32*). Aliquots of purified PrPs in deionized water were stored at −80 °C. The protein concentration used in our experiment was OD_{280} = 0.25. If necessary, the molar concentration was calculated using the molar extinction coefficient ε_{280} according to ExPASy Proteomics Server of the Swiss Institute of Bioinformatics.

Preparation of Lipid Vesicles. The isolation of lipids from N2A cells or mouse brains was described previously (*33*). Other lipids were purchased from Avanti Polar Lipids Inc. For vesicle preparation, lipids in chloroform were dried under a stream of nitrogen at 42 °C and then hydrated in 20 mM Tris-HCl buffer (pH 7.4), yielding a final concentration of 2.5 mg/mL. The hydrated lipids were vortexed and then sonicated in a cup-hold sonicator (Misonix Inc. model XL2020) until they were clear. Prepared lipid vesicles were flushed with argon and stored at 4 °C.

Gradient Analysis. For the discontinuous iodixanol density gradient floatation assay, rPrP and lipid vesicles were mixed together for 10 min at room temperature and applied to the high-density phase of the iodixanol gradient as previously described (*29*, *33*). For high-salt and high-pH extraction, 0.5 M $NaHCO_3$ (pH 11) or a solution of 1.5 M KCl and 10 mM NaOH was added to rPrP/lipid mixtures prior to the gradient analysis. For the salt competition assay, rPrP was pre-equilibrated with various concentrations of KCl for 5 min at room temperature. Immediately before rPrP was mixed with lipids, the same concentrations of KCl were added to the lipid vesicles. The mixed rPrP and lipid solution was incubated at room temperature for 10 min prior to the iodixanol density gradient analysis. Twelve fractions (200 μL/fraction) were collected from top to bottom of the gradient or as indicated.

PrP Lipid Incubation and PK Digestion. For all analyses, rPrP was first subject to a 1 h, 100000*g* centrifugation and only soluble rPrP was used. For rPrP and lipid incubation, 300 μL of rPrP (OD_{280} = 0.25) was mixed with 100 μL of lipid vesicles (2.5 mg/mL). The incubation was conducted at 37 °C for the indicated time periods. For all PK digestions, 10 μL of incubated samples was subjected to PK digestion at 37 °C for 30 min with a PK:rPrP molar ratio of 1:16. The reaction was stopped by addition of 5 mM phenylmethanesulfonyl fluoride (PMSF) and kept on ice for 10 min. One-tenth of PK-digested samples were separated by SDS−PAGE, and the PrP was detected by immunoblot analyses with the POM1 anti-PrP antibody (*34*).

Statistical Analysis. A Student's *t* test was performed for statistical analysis, and the level of significance was set at $p < 0.05$.

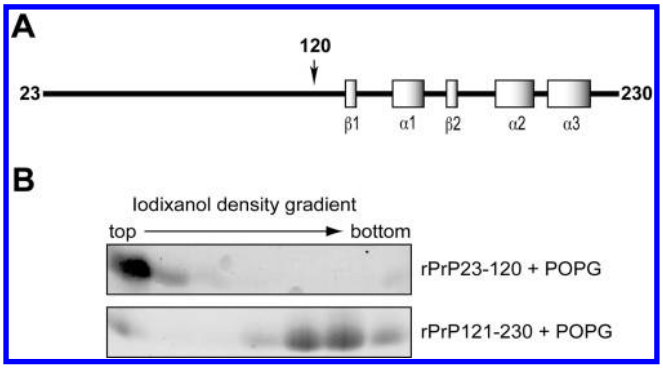

FIGURE 1: N-Terminal fragment of rPrP interacts with anionic lipid. (A) Illustration of mouse rPrP. (B) Iodixanol density gradient analysis of rPrP23−120 with POPG or rPrP121−230 with POPG. Eight fractions (300 μL/fraction) were collected from top to bottom, and the rPrPs were detected by Coomassie Brilliant Blue staining.

RESULTS

The N-Terminal Part of PrP Initiates Electrostatic Interaction between PrP and the Anionic Lipid. Structural studies revealed that the N-terminal part of PrP is flexible and unstructured, while the C-terminal part is well-structured, containing two β-strands and three α-helices (*35*, *36*) (Figure 1A). To determine which part of rPrP is important for its interaction with lipids, we generated two rPrP mutants, the N-terminal rPrP23−120 and the C-terminal rPrP121−230. The mutants were incubated with POPG and then analyzed by the iodixanol gradient. In this discontinuous density gradient, samples were loaded at the bottom, and the lipid-bound protein would migrate to the top of the gradient after ultracentrifugation (*29*, *33*). We found that the N-terminal rPrP23−120 bound strongly to POPG, whereas the majority of the C-terminal rPrP121−230 fragment failed to interact with POPG (Figure 1B). The N-terminal rPrP23−120 contains two clusters of positively charged amino acid residues: one at the very N-terminus (positively charged cluster 1, designated CC1) and the other in the middle region (positively charged cluster 2, designated CC2) (Figure 2A). Therefore, this result is consistent with our previous finding that the PrP−lipid interaction is initiated by electrostatic contact (*29*), suggesting that these positively charged regions are important for the initial electrostatic contact between rPrP and anionic POPG.

The Conserved Hydrophobic Domain of PrP Is Required for Hydrophobic rPrP−Lipid Interaction. In addition to the electrostatic interaction, rPrP also interacts with anionic lipids hydrophobically (*29*). To determine whether the hydrophobic domain (amino acids 111−134) of PrP (Figure 2A) is involved in the hydrophobic lipid−PrP interaction, we generated a mouse rPrP mutant in which the hydrophobic domain was deleted (amino acids 111−131, designated ΔH). To rule out the possibility that the deletion mutant alters the density and interferes with the gradient analysis, we subjected the ΔH mutant to the iodixanol gradient analysis (*29*, *33*). After ultracentrifugation, ΔH remained at the bottom of the gradient, revealing that the hydrophobic domain deletion did not drastically alter the rPrP density (Figure 2B, top). When ΔH was mixed with lipids, it bound to the lipids and migrated to the top of the gradient (Figure 2B, middle). In contrast to wild-type rPrP−lipid interaction (*29*), the ΔH-lipid interaction was almost completely disrupted by the extraction with a high-salt and high-pH solution (Figure 2B, bottom), indicating a significantly weakened hydrophobic interaction.

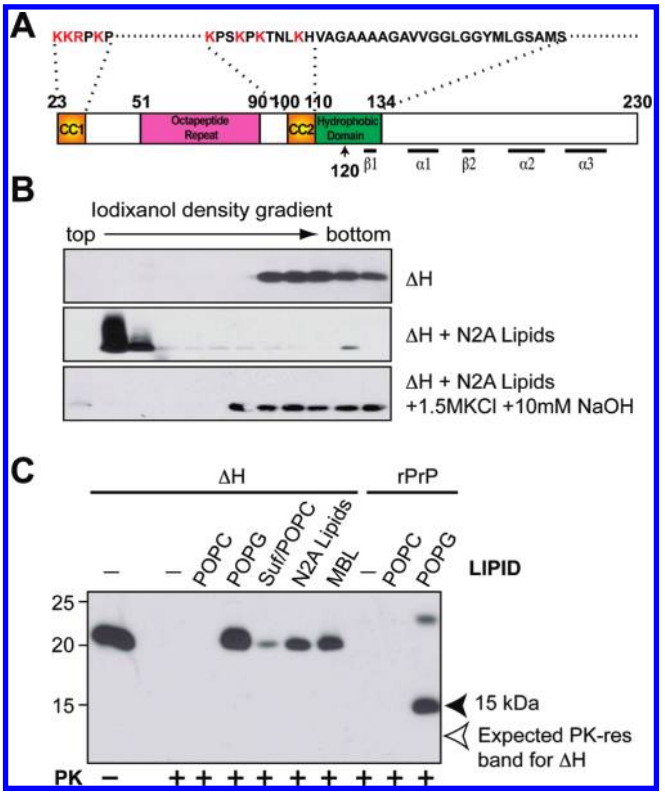

FIGURE 2: Highly conserved hydrophobic domain of PrP required for hydrophobic rPrP−lipid interaction. (A) Illustration of mouse PrP23−230. The amino acids were numbered according to the mouse PrP sequence. (B) Iodixanol density gradient analyses of mouse ΔH alone, ΔH with total lipids isolated from N2A neuroblastoma cells (N2A lipids), and ΔH with N2A lipids extracted with the 1.5 M KCl/10 mM NaOH solution. (C) Mouse rPrP or rPrP ΔH were incubated with the indicated lipids for 1 h and subjected to PK digestion. The filled arrowhead points at the 15 kDa PK-resistant band generated from wild-type rPrP. The empty arrow points at the expected position of the PK-resistant band of rPrP ΔH. Abbreviations: Suf, sulfatide; Suf/POPC, sulfatide and POPC at a mass ratio of 1:1; MBL, mouse brain lipids. PrP was detected by immunoblot analysis with the POM1 antibody.

Next, we determined whether the ΔH mutant was able to gain the lipid-induced C-terminal PK resistance. We previously showed that the anionic lipid interaction causes rPrP to gain different PK-resistant forms (*29*). Because the C-terminal 15 kDa PK-resistant fragment is similar to the PK-resistant core of recombinant prion in size and pattern (*12*), we used it as a marker to monitor the rPrP−lipid interaction and the subsequent conformational change. After incubation with various anionic lipids that are capable of converting rPrP (ref *29* and Figure 2C, last lane), we found that no C-terminal PK-resistant fragment of mutant ΔH was detected in any of the samples (Figure 2C, indicated by an empty arrow).

The POM1 antibody used in this experiment recognizes a discontinuous epitope in the globular domain of PrP (amino acids 121−230) (*34*). The ΔH mutant deleted a fragment within this region, raising the possibility that the lack of the C-terminal PK-resistant band was due to the loss of the POM1 epitope. To rule out this possibility, we performed immunoblot analysis with the 8H4 antibody, which has a more defined C-terminal epitope (amino acids 175−195) outside of the hydrophobic domain. Our result verified that the lack of C-terminal PK-resistant rPrP fragment was not due to the loss of the POM1 epitope (data not shown). Together, our results support the possibility that the

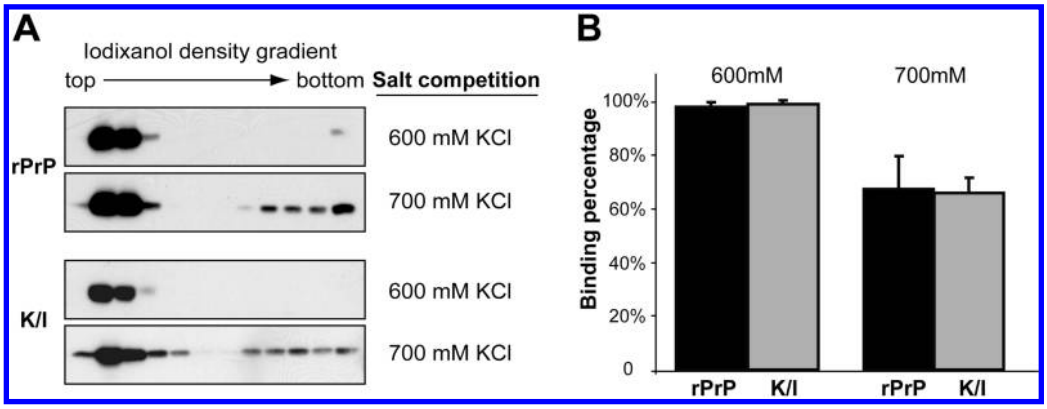

FIGURE 3: Positively charged lysine residues in the middle region do not affect electrostatic interaction between rPrP and anionic lipids. (A) Salt competition assays for wild-type rPrP and the K/I mutant. The rPrPs and POPG were pre-equilibrated with KCl at the indicated concentrations and then mixed together. After a 10 min incubation at room temperature, rPrP/lipid mixtures were subjected to iodixanol density gradient separation. PrP was detected by immunoblot analysis with the POM1 antibody. (B) Densitometric analyses of results shown in panel A. The density sum of all 12 fractions in each experiment was used as the total amount of rPrP, and the density sum of the first six fractions was used as the amount of lipid-bound rPrP. The binding assays were repeated three times for each sample under the indicated conditions. The error bar represents the standard deviation.

hydrophobic domain of PrP is required for the hydrophobic rPrP−lipid interaction, which is important for rPrP to gain C-terminal PK resistance.

Although the C-terminal PK-resistant form was not detected, various levels of full-length PK-resistant ΔH were detected in samples incubated with anionic lipids, but not in control samples in which ΔH was incubated with or without zwitterionic POPC (1-palmitoyl-2-oleoyl-*sn*-glycero-3-phosphocholine) (Figure 2C). On the basis of the fact that ΔH was completely digested in control samples and wild-type rPrP exhibited a correct PK-resistant pattern after incubation with anionic POPG (Figure 2C, last lane) (*29*), we concluded that the appearance of full-length PK-resistant ΔH was not due to insufficient PK digestion. Actually, the separation of full-length and C-terminal PK-resistant forms in these samples and in experiments described below (Figure 4B) supports the possibility that, as we previously suggested (*29*), these are different rPrP forms that resulted from the rPrP−lipid interaction.

Middle Region-Localized Lysine Residues Affect rPrP−Lipid Interaction. The finding that the hydrophobic domain plays an important role in rPrP−lipid interaction led us to predict that CC2 (Figure 2A), a positively charged region immediately preceding the hydrophobic domain, will likely modulate rPrP−lipid interaction. To test this hypothesis, we generated a mouse rPrP mutant in which all four lysine residues in CC2 (residues 100, 103, 105, and 109 of mouse PrP) were replaced with isoleucine (designated K/I). Taking advantage of the fact that high concentrations of salt inhibit the initial electrostatic rPrP−lipid contact (*29*), we performed a salt competition analysis to compare the strength of electrostatic rPrP−lipid interaction between wild-type and mutant rPrPs. In the presence of 600 mM KCl, the majority of wild-type rPrP bound to POPG. When the salt concentration increased to 700 mM KCl, only ~70% of rPrP remained lipid-bound (Figure 3A, top panels, and Figure 3B). Interestingly, although the K/I mutant lost quite a few positive charges, the pattern of the K/I mutant binding to POPG was similar to that of wild-type rPrP in the salt competition assay (Figure 3). This result indicates that the loss of positive charges in CC2 does not significantly alter the strength of electrostatic rPrP−lipid interaction.

When the K/I mutant−lipid complex was extracted with a high-salt and high-pH solution, the K/I mutant remained lipid-bound and migrated to the top fractions (Figure 4A), suggesting

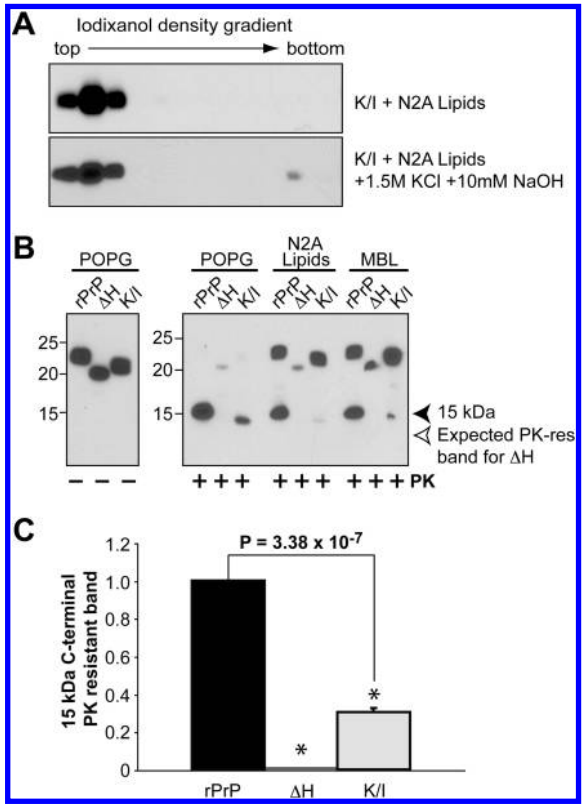

FIGURE 4: Middle region-localized lysine residues affect the lipid-induced rPrP conformational change. (A) Iodixanol density gradient analysis of mouse K/I with N2A lipids or K/I with N2A lipids extracted with a 1.5 M KCl/10 mM NaOH solution as indicated. (B) Wild-type mouse rPrP, ΔH, or K/I was incubated with the indicated lipids for 1 h and subjected to PK digestion. MBL denotes mouse brain lipids. PrP was detected by immunoblot analysis with the POM1 antibody. (C) Densitometric analysis of the 15 kDa PK-resistant band. The density of the 15 kDa band generated by rPrP incubated with POPG was set as 1. The density of the 15 kDa band generated by ΔH or K/I incubated with POPG was used to calculate the PK resistance. The PK digestion assay was repeated three times for each sample. The error bar represents the standard deviation, and the asterisk indicates a significant difference.

a hydrophobic interaction between the K/I mutant and lipids. Intriguingly, while the elimination of these four lysine residues did not seem to alter the strength of electrostatic or hydrophobic

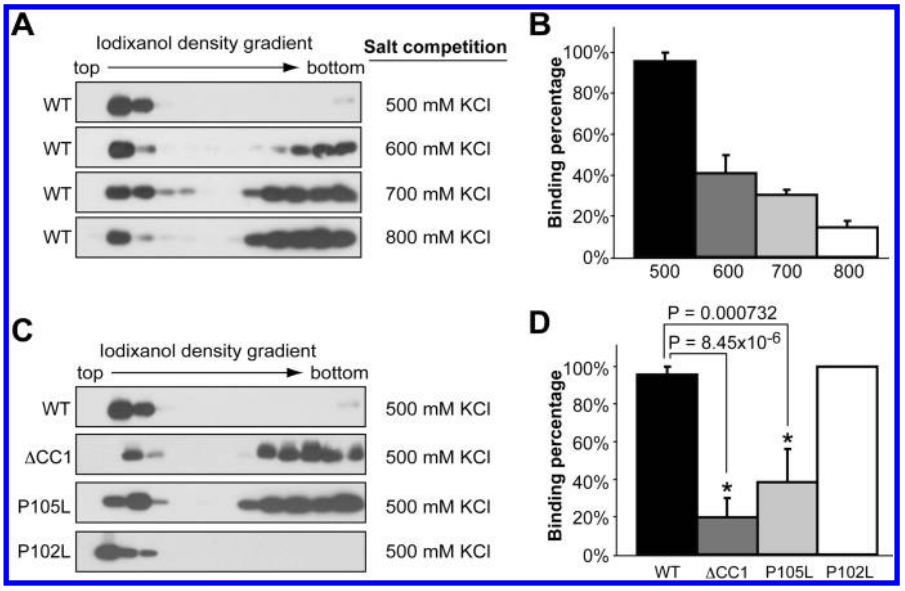

FIGURE 5: Middle region-localized P105L and P102L mutations and positive charges at the N-terminus have different effects on electrostatic rPrP−lipid interaction. (A) Salt competition assays for wild-type human rPrP incubated with POPG in the presence of the indicated salt concentrations. After binding, the POPG−rPrP complex was separated by the iodixanol density gradient. (B) Densitometric analyses of the results in panel A. (C) Salt competition assays for human rPrP mutants ΔCC1, P105L, and P102L incubated with POPG in the presence of 500 mM KCl. PrP was detected by immunoblot analysis with the POM1 antibody. (D) Densitometric analyses of the results in panel C. For densitometric analyses, the density sum of all 12 fractions in each experiment was used as the total amount of rPrP, and the density sum of the first six fractions was used as the amount of lipid-bound rPrP. The binding assays were repeated three times for each sample. The error bar represents the standard deviation, and the asterisk indicates a significant difference.

lipid−rPrP interaction, it did significantly reduce the lipid-induced C-terminal PK-resistant rPrP (Figure 4B,C). This finding suggests that the lysine residues in CC2 modulate the rPrP−lipid interaction in such a manner that it assists in the generation of the C-terminal PK-resistant rPrP form.

Disease-Associated P105L and P102L Mutations and the N-Terminal Positively Charged Region Affect rPrP−Lipid Interaction in Different Manners. To determine the influence of disease-associated mutation and the N-terminal positively charged region on rPrP−lipid interaction, we analyzed two CC2-localized disease-associated mutations, P102L and P105L, and a PrP mutant without CC1, the very N-terminal positively charged amino acid cluster (amino acids 23−27 deleted, designated ΔCC1). Because P102L and P105L are mutations causing human disease, these mutants were made with recombinant human PrP, and wild-type human rPrP (designated rhPrP) was included as a control to assess the influence of these mutations.

First, we performed the salt competition assay with rhPrP. The majority of rhPrP bound to POPG in the presence of 500 mM KCl, and increasing salt concentrations of > 500 mM reduced the amounts of lipid-bound rhPrP (Figure 5A,B). Next, we analyzed the lipid binding ability of various rhPrP mutants in the presence of 500 mM KCl. As expected, a significant portion of the ΔCC1 mutant failed to bind POPG in the presence of 500 mM KCl [Figure 5C, second panel, and Figure 5D ($p = 8.45 \times 10^{-6}$)], which is likely because of its reduced positive charges at the N-terminus. Surprisingly, the P105L mutant, which retains all the positively charged amino acids, exhibited significantly weakened POPG binding as well [Figure 5C, third panel, and Figure 5D ($p = 0.000732$)]. In contrast, the P102L mutant, which is only three amino acids upstream and has exactly the same amino acid replacement as the P105L mutant, bound to POPG as strong as rhPrP (Figure 5C, fourth panel, and Figure 5D).

Despite different behaviors in the salt competition assay, all mutants were 100% POPG-bound at the physiological salt concentration (data not shown). Moreover, they remained lipid-bound after extraction with a high-salt and high-pH solution (Figure 6A). This result indicates that these mutations do not significantly affect the strength of hydrophobic rPrP−lipid interaction.

PK digestion was performed to analyze the influence of these mutations on lipid-induced C-terminal PK resistance, and dramatic differences were observed (Figure 6B). After a 1 h incubation with POPG at the physiological salt concentration (150 mM NaCl), the ΔCC1 mutant generated a similar amount of the 15 kDa C-terminal PK-resistant fragment as wild-type PrP [Figure 6B, +PK (equal amounts of rhPrP input were verified by immunoblot analysis with samples without PK digestion), and Figure 6B, −PK]. However, a much weaker 15 kDa PK-resistant band was detected with the P105L mutant under the same conditions [Figure 6B,C ($p = 4.06 \times 10^{-9}$)], while the amount of a PK-resistant fragment with a slightly lower molecular mass (~14 kDa) was increased. Surprisingly, the P102L mutant, which interacts with lipids like wild-type PrP, completely failed to generate any PK-resistant band (Figure 6B,C). Together with lipid binding data, these results suggest that both the positively charged CC1 and CC2 regions contribute to rPrP−lipid interaction, yet the generation of the C-terminal PK-resistant rPrP form is mainly influenced by how CC2 interacts with lipids.

The Middle Region-Localized 129 Polymorphism Affects rPrP−Lipid Interaction. The 129 ploymorphism, which is localized in the hydrophobic domain, has a significant influence on the pathogenesis of prion disease (*37*). We tested its influence on rPrP−lipid interaction by generating recombinant human PrP with either methionine or valine at residue 129 (designated 129M or 129V, respectively). The salt competition assay was performed with POPG or mixed lipids isolated from mouse brain (MBL). When POPG was used, almost 100% of 129M and 129V were lipid-bound in the presence of 500 mM KCl (Figure 5A and data not shown). When MBL was used, the overall ability of rhPrP to

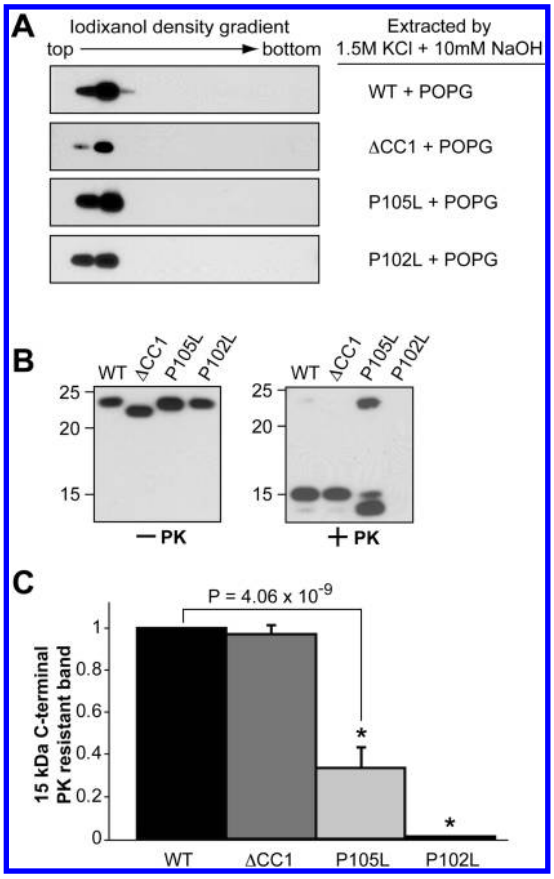

FIGURE 6: The influence of disease-associated P105L and P102L mutations and the N-terminal positively charged region on lipid-induced rPrP conformational change in different manners. (A) Wild-type human rPrP, ΔCC1, P105L, or P102L was incubated with POPG and then extracted with an alkaline solution of 1.5 M KCl and 10 mM NaOH prior to the iodixanol density gradient analysis. (B) Wild-type human rPrP, ΔCC1, P105L, or P102L was incubated with POPG for 1 h and subjected to PK digestion. PrP was detected by immunoblot analysis with the POM1 antibody. (C) Densitometric analyses of the PK digestion results in panel B. The density of the 15 kDa PK-resistant band of wild-type rPrP was set as 1. The density of the 15 kDa band of ΔCC1, P105L, or P102L was used to calculate the PK resistance. The PK digestion assay was repeated three times for each sample. The error bar represents the standard deviation, and the asterisk indicates a significant difference.

bind MBL was weakened (comparing Figure 7A and Figure 5A), and some rhPrP remained at the bottom of the gradient. However, no significant difference was observed between 129M and 129V, suggesting that the 129 polymorphism does not significantly alter the strength of electrostatic rPrP−lipid interaction (Figure 7A,B). The high-salt and high-pH extraction analysis was performed to determine whether the 129 polymorphism alters the strength of hydrophobic rhPrP−lipid interaction. While no difference was observed when POPG was used (data not shown), a significant difference between 129M and 129V was detected when the rhPrP−MBL complexes were extracted with 0.5 M $NaHCO_3$ (pH 11.0). As shown in Figure 7C, a significant portion of 129V was extracted from the complex, while the majority of 129M remained lipid-bound [Figure 7C,D (p = 0.003258)]. This result suggested that the 129 polymorphism alters the hydrophobic strength of binding of rPrP to certain types of lipids.

DISCUSSION

The significance of PrP−lipid interaction in the pathogenesis of prion disease has been elucidated by previous studies (*17*−*21*). The successful conversion of rPrP into a highly infectious prion in the presence of lipids (*12*) supports an important role for the PrP−lipid interaction in this process. We previously showed that the anionic lipid−PrP interaction is mediated by both electrostatic and hydrophobic contacts and that the lipid interaction converts rPrP into a conformation with a 15 kDa C-terminal PK-resistant fragment. The efficiency of lipid-induced rPrP conversion depends on the structure of lipid headgroups and/or the presentation of these headgroups on the surface of lipid vesicles (*29*). In this study, we analyzed PrP domains involved in the PrP−lipid interaction and revealed different roles of the N-terminal and middle regions of PrP. Moreover, our results for disease-associated P102L and P105L mutations and the 129 polymorphism are consistent with the notion that the PrP−lipid interaction plays a role in the pathogenesis of prion disease.

Our results for the salt competition study of wild-type and ΔCC1 mutant PrPs (Figure 5C,D) clearly showed that the N-terminal positively charged region is involved in the electrostatic interaction. The fact that the ΔCC1 mutant behaves like wild-type PrP during high-salt and high-pH extraction and in PK digestion experiments (Figure 6A,B) indicates that the N-terminal CC1 region does not significantly contribute to the hydrophobic PrP−lipid interaction and the subsequent conformational change in PrP, supporting the idea that the lipid-induced PrP conformational change mainly involves the middle and C-terminal parts of PrP (*38*).

The highly conserved middle region contains a cluster of four positively charged lysine residues and a hydrophobic domain (*39*, *40*). The ΔH mutant analyses suggest that the hydrophobic domain is the major PrP domain responsible for the hydrophobic PrP−lipid interaction. Moreover, the inability of the ΔH mutant to gain C-terminal PK resistance after incubation with a variety of anionic lipids (Figures 2C and 4B) suggests that the hydrophobic PrP−lipid interaction is essential for its conversion to the PK-resistant form. In addition to the hydrophobic domain, our results also reveal that the four lysine residues in the CC2 region influence the PrP conformational change. The K/I mutant significantly reduced the amount of lipid-induced C-terminal PK resistance (Figure 4B). Both middle region-localized P102L and P105L mutants reduced the amount of the C-terminal PK-resistant form (Figure 6B). Notably, proline residues at positions 102 and 105 are flanked by lysine residues in the middle region. Because proline is conformationally restrained, the replacement of proline with leucine would alter the presentation of positively charged lysine residues. Together, our results suggest that the four lysine residues in the CC2 region are crucial in orienting the hydrophobic PrP−lipid contact in such a manner that leads rPrP to convert to the C-terminal PK-resistant conformation.

The reduced C-terminal PK-resistant bands associated with the P102L and P105L mutations are consistent with several previous reports of P105L-associated GSS cases or transgenic mice expressing the P102L mutant, which showed severe neurodegeneration without a detectable amount of PK-resistant PrP (*41*−*43*). The toxic mechanism of these mutations may involve disruptions in normal PrP folding, in PrP metabolism, or in PrP's interaction with other ligands for its normal function. Our results, that these two mutants differ drastically from wild-type PrP in lipid interaction, may suggest a role for the PrP−lipid interaction in these processes.

Some paradoxical results were obtained via comparison of the K/I mutant and the P102L or P105L mutant. The K/I mutant,

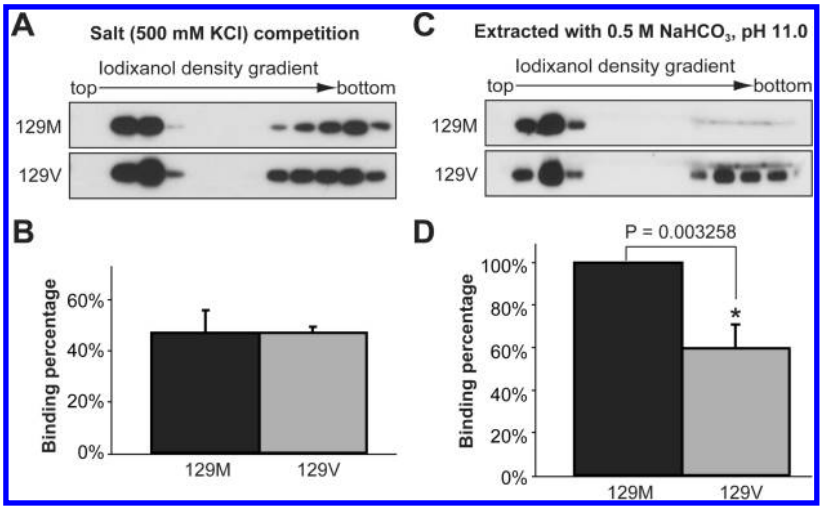

FIGURE 7: Middle region-localized 129 polymorphism affects hydrophobic rPrP−lipid interaction. (A) Salt competition assay for human rPrP 129M or 129V incubated with mouse brain lipids (MBL) in the presence of 500 mM KCl. (B) Densitometric analyses of the results in panel A. (C) Human rPrP 129M−MBL or 129V−MBL complex extracted with a 0.5 M $NaHCO_3$ solution (pH 11.0) prior to the iodixanol density gradient analysis. PrP was detected by immunoblot analysis with the POM1 antibody. (D) Densitometric analyses of the results in panel C. For densitometric analysis, the density sum of all 12 fractions in each experiment was used as the total amount of rPrP, and the density sum of the first six fractions was used as the amount of lipid-bound rPrP. The binding assays were repeated three times for each sample. The error bar represents the standard deviation, and the asterisk indicates a significant difference.

with all four middle region-localized lysines mutated, did not appear to alter the strength of either the electrostatic or hydrophobic PrP−lipid interaction (Figures 3A and 4A). However, the P105L mutant did significantly alter the strength of electrostatic PrP−lipid interaction (Figure 5C). Moreover, although the P102L mutant did not alter the rPrP−lipid binding properties in our assays (Figure 5C), it completely failed to convert to the PK-resistant form (Figure 6B). However, with the K/I and P105L mutants, the magnitude of the 15 kDa C-terminal PK-resistant band was reduced, but still detectable (Figures 4B and 6B). These paradoxical results suggest that, besides their effects on flanking lysine residues, the P105L and P102L mutations likely have an impact on the global structure of rPrP as well (*30*), which could affect the binding of rPrP to lipid or the lipid-induced rPrP conformation. Nevertheless, our results clearly reveal the importance of the CC2 region in PrP−lipid interaction and in lipid-induced PrP conversion.

The 129 polymorphism, localized in the hydrophobic domain, significantly affects the susceptibility and pathogenesis of prion disease (*37*). However, structural studies revealed similar conformation and stability between PrP variants with an M or a V at position 129 (*44*), suggesting that it is not their influence on PrP structure but rather their differences in interacting with other ligands that may contribute to the different pathogenic changes. We found that the M and V variants differ in their hydrophobic interactions with lipids, and a stronger hydrophobic interaction was detected for 129M (Figure 7C,D). Although valine is more hydrophobic than methionine, the hydrophobic PrP−lipid interaction does not rely on only residue 129 but involves multiple hydrophobic amino acids. Substituting methionine with valine increases the hydrophobicity and likely causes a tighter interaction between residue 129 and fatty acyl chains. The tight lipid interaction at residue 129 could alter the interaction between lipids and other surrounding hydrophobic amino acids. As a result, the total strength of the hydrophobic lipid interaction is reduced for 129V.

Collectively, our results provide novel insights into the PrP−lipid interaction and indicate a significant role of the highly conserved middle region in lipid-induced PrP conversion. The fact that disease-associated mutations and the 129 polymorphism significantly alter PrP−lipid interaction supports the relevance of PrP−lipid interaction in the pathogenesis of prion disease.

ACKNOWLEDGMENT

We thank Dr. Adriano Aguzzi for providing the POM1 antibody and Kate Lorenzetti for proofreading the manuscript.

REFERENCES

1. Prusiner, S. B. (1998) Prions. *Proc. Natl. Acad. Sci. U.S.A. 95*, 13363–13383.
2. Caughey, B., and Chesebro, B. (1997) Prion protein and the transmissible spongiform encephalopathies. *Trends Cell Biol. 7*, 56–62.
3. Watts, J. C., Balachandran, A., and Westaway, D. (2006) The expanding universe of prion diseases. *PLoS Pathog. 2*, e26.
4. Collinge, J. (2001) Prion diseases of humans and animals: Their causes and molecular basis. *Annu. Rev. Neurosci. 24*, 519–550.
5. Aguzzi, A. (2006) Prion diseases of humans and farm animals: Epidemiology, genetics, and pathogenesis. *J. Neurochem. 97*, 1726–1739.
6. Caughey, B., and Baron, G. S. (2006) Prions and their partners in crime. *Nature 443*, 803–810.
7. Cohen, F. E., and Prusiner, S. B. (1998) Pathologic conformations of prion proteins. *Annu. Rev. Biochem. 67*, 793–819.
8. Baskakov, I. V., and Breydo, L. (2007) Converting the prion protein: What makes the protein infectious. *Biochim. Biophys. Acta 1772*, 692–703.
9. Collinge, J., and Clarke, A. R. (2007) A general model of prion strains and their pathogenicity. *Science 318*, 930–936.
10. Aguzzi, A., Baumann, F., and Bremer, J. (2008) The prion's elusive reason for being. *Annu. Rev. Neurosci. 31*, 439–477.
11. Caughey, B., Baron, G. S., Chesebro, B., and Jeffrey, M. (2009) Getting a grip on prions: Oligomers, amyloids, and pathological membrane interactions. *Annu. Rev. Biochem. 78*, 177–204.
12. Wang, F., Wang, X., Yuan, C. G., and Ma, J. (2010) Generating a prion with bacterially expressed recombinant prion protein. *Science 327*, 1132–1135.
13. Supattapone, S. (2010) Biochemistry. What makes a prion infectious? *Science 327*, 1091–1092.
14. Deleault, N. R., Lucassen, R. W., and Supattapone, S. (2003) RNA molecules stimulate prion protein conversion. *Nature 425*, 717–720.
15. Deleault, N. R., Geoghegan, J. C., Nishina, K., Kascsak, R., Williamson, R. A., and Supattapone, S. (2005) Protease-resistant prion protein amplification reconstituted with partially purified substrates and synthetic polyanions. *J. Biol. Chem. 280*, 26873–26879.

16. Deleault, N. R., Harris, B. T., Rees, J. R., and Supattapone, S. (2007) Formation of native prions from minimal components in vitro. *Proc. Natl. Acad. Sci. U.S.A. 104*, 9741–9746.
17. Klein, T. R., Kirsch, D., Kaufmann, R., and Riesner, D. (1998) Prion rods contain small amounts of two host sphingolipids as revealed by thin-layer chromatography and mass spectrometry. *Biol. Chem. 379*, 655–666.
18. Gabizon, R., McKinley, M. P., and Prusiner, S. B. (1987) Purified prion proteins and scrapie infectivity copartition into liposomes. *Proc. Natl. Acad. Sci. U.S.A. 84*, 4017–4021.
19. Baron, G. S., Magalhaes, A. C., Prado, M. A., and Caughey, B. (2006) Mouse-adapted scrapie infection of SN56 cells: Greater efficiency with microsome-associated versus purified PrP-res. *J. Virol. 80*, 2106–2117.
20. Taraboulos, A., Scott, M., Semenov, A., Avrahami, D., Laszlo, L., and Prusiner, S. B. (1995) Cholesterol depletion and modification of COOH-terminal targeting sequence of the prion protein inhibit formation of the scrapie isoform. *J. Cell Biol. 129*, 121–132.
21. Naslavsky, N., Shmeeda, H., Friedlander, G., Yanai, A., Futerman, A. H., Barenholz, Y., and Taraboulos, A. (1999) Sphingolipid depletion increases formation of the scrapie prion protein in neuroblastoma cells infected with prions. *J. Biol. Chem. 274*, 20763–20771.
22. Baron, G. S., and Caughey, B. (2003) Effect of glycosylphosphatidylinositol anchor-dependent and -independent prion protein association with model raft membranes on conversion to the protease-resistant isoform. *J. Biol. Chem. 278*, 14883–14892.
23. Morillas, M., Swietnicki, W., Gambetti, P., and Surewicz, W. K. (1999) Membrane environment alters the conformational structure of the recombinant human prion protein. *J. Biol. Chem. 274*, 36859–36865.
24. Sanghera, N., and Pinheiro, T. J. (2002) Binding of prion protein to lipid membranes and implications for prion conversion. *J. Mol. Biol. 315*, 1241–1256.
25. Kazlauskaite, J., Sanghera, N., Sylvester, I., Venien-Bryan, C., and Pinheiro, T. J. (2003) Structural changes of the prion protein in lipid membranes leading to aggregation and fibrillization. *Biochemistry 42*, 3295–3304.
26. Critchley, P., Kazlauskaite, J., Eason, R., and Pinheiro, T. J. (2004) Binding of prion proteins to lipid membranes. *Biochem. Biophys. Res. Commun. 313*, 559–567.
27. Luhrs, T., Zahn, R., and Wuthrich, K. (2006) Amyloid formation by recombinant full-length prion proteins in phospholipid bicelle solutions. *J. Mol. Biol. 357*, 833–841.
28. Elfrink, K., Ollesch, J., Stohr, J., Willbold, D., Riesner, D., and Gerwert, K. (2008) Structural changes of membrane-anchored native PrP^{C}. *Proc. Natl. Acad. Sci. U.S.A. 105*, 10815–10819.
29. Wang, F., Yang, F., Hu, Y., Wang, X., Jin, C., and Ma, J. (2007) Lipid interaction converts prion protein to a PrPSc-like proteinase K-resistant conformation under physiological conditions. *Biochemistry 46*, 7045–7053.
30. Yin, S., Pham, N., Yu, S., Li, C., Wong, P., Chang, B., Kang, S. C., Biasini, E., Tien, P., Harris, D. A., and Sy, M. S. (2007) Human prion proteins with pathogenic mutations share common conformational changes resulting in enhanced binding to glycosaminoglycans. *Proc. Natl. Acad. Sci. U.S.A. 104*, 7546–7551.
31. Zahn, R., von Schroetter, C., and Wuthrich, K. (1997) Human prion proteins expressed in *Escherichia coli* and purified by high-affinity column refolding. *FEBS Lett. 417*, 400–404.
32. Yin, S. M., Zheng, Y., and Tien, P. (2003) On-column purification and refolding of recombinant bovine prion protein: Using its octarepeat sequences as a natural affinity tag. *Protein Expression Purif. 32*, 104–109.
33. Wang, X., Wang, F., Arterburn, L., Wollmann, R., and Ma, J. (2006) The interaction between cytoplasmic prion protein and the hydrophobic lipid core of membrane correlates with neurotoxicity. *J. Biol. Chem. 281*, 13559–13565.
34. Polymenidou, M., Stoeck, K., Glatzel, M., Vey, M., Bellon, A., and Aguzzi, A. (2005) Coexistence of multiple PrPSc types in individuals with Creutzfeldt-Jakob disease. *Lancet Neurol. 4*, 805–814.
35. Riek, R., Hornemann, S., Wider, G., Billeter, M., Glockshuber, R., and Wuthrich, K. (1996) NMR structure of the mouse prion protein domain PrP(121−321). *Nature 382*, 180–182.
36. Riek, R., Hornemann, S., Wider, G., Glockshuber, R., and Wuthrich, K. (1997) NMR characterization of the full-length recombinant murine prion protein, mPrP(23−231). *FEBS Lett. 413*, 282–288.
37. Ironside, J. W., Ritchie, D. L., and Head, M. W. (2005) Phenotypic variability in human prion diseases. *Neuropathol. Appl. Neurobiol. 31*, 565–579.
38. Cobb, N. J., Sonnichsen, F. D., McHaourab, H., and Surewicz, W. K. (2007) Molecular architecture of human prion protein amyloid: A parallel, in-register β-structure. *Proc. Natl. Acad. Sci. U.S.A. 104*, 18946–18951.
39. Hegde, R. S., Mastrianni, J. A., Scott, M. R., DeFea, K. A., Tremblay, P., Torchia, M., DeArmond, S. J., Prusiner, S. B., and Lingappa, V. R. (1998) A transmembrane form of the prion protein in neurodegenerative disease. *Science 279*, 827–834.
40. Aguzzi, A., Sigurdson, C., and Heikenwaelder, M. (2008) Molecular mechanisms of prion pathogenesis. *Annu. Rev. Pathol. 3*, 11–40.
41. Telling, G. C., Haga, T., Torchia, M., Tremblay, P., DeArmond, S. J., and Prusiner, S. B. (1996) Interactions between wild-type and mutant prion proteins modulate neurodegeneration in transgenic mice. *Genes Dev. 10*, 1736–1750.
42. Yamada, M., Itoh, Y., Inaba, A., Wada, Y., Takashima, M., Satoh, S., Kamata, T., Okeda, R., Kayano, T., Suematsu, N., Kitamoto, T., Otomo, E., Matsushita, M., and Mizusawa, H. (1999) An inherited prion disease with a PrP P105L mutation: Clinicopathologic and PrP heterogeneity. *Neurology 53*, 181–188.
43. Collins, S., McLean, C. A., and Masters, C. L. (2001) Gerstmann-Straussler-Scheinker syndrome, fatal familial insomnia, and kuru: A review of these less common human transmissible spongiform encephalopathies. *J. Clin. Neurosci. 8*, 387–397.
44. Hosszu, L. L., Jackson, G. S., Trevitt, C. R., Jones, S., Batchelor, M., Bhelt, D., Prodromidou, K., Clarke, A. R., Waltho, J. P., and Collinge, J. (2004) The residue 129 polymorphism in human prion protein does not confer susceptibility to Creutzfeldt-Jakob disease by altering the structure or global stability of PrPC. *J. Biol. Chem. 279*, 28515–28521.